

Examining patch and landscape-level white-tailed deer connectivity using a novel, buffer and resistance-based metric

Collin O'Connor

Collin.OConnor@health.ny.gov

New York State Department of Health

Jared Aldstadt

University at Buffalo

Adam Wilson

University at Buffalo

Research Article

Keywords: Functional connectivity, Structural connectivity, White-tailed deer, Least-cost-paths, Probability of Connectivity, New York State

Posted Date: July 22nd, 2024

DOI: <https://doi.org/10.21203/rs.3.rs-4655632/v1>

License:  This work is licensed under a Creative Commons Attribution 4.0 International License.

[Read Full License](#)

Additional Declarations: No competing interests reported.

Abstract

Context: Landscape connectivity drives many ecological processes and can be quantified using numerous metrics. Few metrics can be interpreted at both patch and landscape-levels, incorporate structural and functional connectivity, and are computationally efficient.

Objectives: We sought a generalizable connectivity metric for individual patches and landscapes. An ideal metric could accurately estimate the functional connectivity of white-tailed deer (*Odocoileus virginianus*).

Methods: The Sinuous Connection Reduction (SCR) index is a functional connectivity metric modified from the Probability of Connectivity (PC) index and Equivalent Connected Area (ECA). SCR is calculated by adding patch area between adjacent patches, where the area added is reduced by a factor of the inverse of least-cost-path sinuosity between the patches. A case-study calculates SCR, PC, and ECA for white-tailed deer in NYS, and metrics are compared to historical counts of deer take.

Results: SCR can be calculated for individual patches and landscapes, providing a hierarchical understanding of connectivity. Spatial panel regression models indicate ECA is the best fitting metric for white-tailed deer connectivity, followed by SCR and PC. Both PC and ECA are susceptible to boundary effects, and ECA values are partially attributed to landscape size. Geographically weighted regression models indicate opposing relationships between metrics and deer take in different regions of NYS, indicating deer populations are modulated by other locationally-specific factors apart from connectivity.

Conclusions: SCR can be considered useful over PC when home-ranges apply, though it requires data-intensive least-cost path modeling. SCR is computationally efficient when modeling landscapes with many disjointed patches and incorporates both functional and structural connectivity.

Introduction

Landscape heterogeneity and fragmentation is an important feature that influences the stability of meta-populations, i.e., spatially separated sub-populations that interact with each other. (Levins, 1969). The concept of connectivity arose to assess how sub-populations within a fragmented landscape are interconnected as a single population via their dispersal between patches (Merriam, 1984). Landscape connectivity was later defined as, “the degree to which the landscape facilitates or impedes movement among resource patches.” (Taylor et al., 1993). Under this framework, resource patches are generally depicted as a mosaic of polygons separated by a resource-devoid landscape (Dunning et al., 1992; D. L. Urban et al., 1987). Landscape connectivity can generally be subdivided into structural connectivity and functional connectivity (Keeley et al., 2021). Structural connectivity describes the landscape with respect to the pattern of the mosaic, typically without the added context of how specific organisms navigate such a landscape (Metzger & Décamps, 1997). Conversely, functional connectivity incorporates and assesses ecological outcomes of connectivity. Fahrig et al. (2021) further defines structural connectivity as Noss connectivity and subdivides functional connectivity into Merriam connectivity and Hanski

connectivity. In this formulation, Merriam connectivity is concerned with the movement potential of a particular organism between the habitat patches in a mosaic, while Hanski connectivity is concerned with an organism's population success (Baudry & Merriam, 1988; Fahrig et al., 2021; Hanski, 1994; Merriam, 1984; Moilanen & Hanski, 1998; Noss, 1987). Though functional and structural connectivity can be estimated separately, both are necessary to incorporate a consistent definition of landscape connectivity and remain biologically useful (Fahrig et al., 2021; Saura & Pascual-Hortal, 2007; Tischendorf & Fahrig, 2000b, 2000a).

Estimates of landscape connectivity are determined using various metrics, each with its own data requirements and configuration parameters. (Keeley et al., 2021). A summary by Keeley et al (2021) lays out a framework where landscape connectivity metrics can be binned into those that measure structural connectivity, functional connectivity, or a combination of both. Landscape metrics measuring functional connectivity are typically those that incorporate species-specific components of population dynamics, particularly the movement of a species between habitat patches (Merriam connectivity) or the overall population success (Hanski connectivity) (Fahrig et al., 2021; Keeley et al., 2021; Tischendorf & Fahrig, 2000b). Two of the most important functional connectivity metrics are patch occupancy and between-patch dispersal, which have been used for over two decades to estimate landscape connectivity (Dieckmann et al., 1999; Inglis & Underwood, 1992). Between-patch gene-flow is also informative both as a measure for between-patch dispersal and for assessing population and meta-population health (Bossart & Pashley Prowell, 1998; Horskins et al., 2006; Vos et al., 2001; Waser & Strobeck, 1998; Whitlock & McCauley, 1999).

Unlike functional connectivity metrics, structural connectivity metrics assess connectivity by incorporating the physical arrangement of habitat within a landscape (Keeley et al., 2021). Reasonably, an ideal structural connectivity metric should incorporate qualities of a landscape that consistently scale with an increase or decrease of the metric (Saura & Pascual-Hortal, 2007).

Moilanen and Nieminen (2002) lay out a series of simple structural connectivity metrics that can be calculated at low computational cost. Two examples of patch-level structural connectivity metrics include the percent of habitat within a buffer area and area-weighted isolation of a focal patch, i.e., the distance between a patch and its nearest neighbor weighted by their respective areas. Notably, simple structural connectivity metrics can lack species-specific predictability; habitat patch area and distance to the nearest patch have been shown to provide opposing estimates of dispersal success (Moilanen & Nieminen, 2002; Tischendorf & Fahrig, 2000a). More advanced structural connectivity landscape metrics often operationalize graph theory, where a landscape is discretized into a series of nodes (representing habitat patches) and edges (representing some links between the nodes) (D. Urban & Keitt, 2001). Examples of graph-based metrics include: Harary index, Degree of Connectedness, Integral Index of Connectivity (IIC), Graph diameter, and Compartmentalization (Minor & Urban, 2008; Pascual-Hortal & Saura, 2006; Ricotta et al., 2000; D. Urban & Keitt, 2001). Additional examples are described in Keeley et al (2021) and Pascual-Hortal and Saura (2006).

Metrics that incorporate elements of structural connectivity (patch area and pattern of mosaic) and functional connectivity (biological or ecological properties) are categorized in Keeley et al (2021) as “both”. Some of these metrics utilize graph-theoretic approaches combined with species-specific movement or dispersal cutoff rules, including: the Probability of Connectivity index, Equivalent Connected Area, and ProtConn indicator (Saura et al., 2011, 2017, 2018; Saura & Pascual-Hortal, 2007). The Probability of Connectivity (PC) index is calculated from a graph of all patches and links within a landscape, including the area of all patches and the probability of dispersal between all between-patch links (Saura & Pascual-Hortal, 2007). In its most basic form, the PC index is inherently a structural connectivity metric, however, species-specific behaviors can be directly parameterized. (Bunn et al., 2000; Saura et al., 2011; Saura & Pascual-Hortal, 2007). Metrics that are classified as both structural and functional connectivity metrics also include resistance-based metrics, which operate by calculating a species-specific response to the state of a landscape in the form of raster cells (Keeley et al., 2021). Such metrics benefit from incorporating theoretical species-movement directly, without the need for experimentally collected data. Specifically, least-cost-path modeling uses resistance surfaces and search algorithms to calculate the most likely path a species will take between two nodes, though this method is computationally intensive (Bunn et al., 2000; Dijkstra, 1959; D. L. Urban et al., 2009). Current Flow Centrality and Current Density are resistance-based metrics often used to categorize individual raster cells for use in visualization for specific linkage paths (Dickson et al., 2017; McRae et al., 2008; VanAcker et al., 2019). The General Ecological Connectivity Index uses an “impedance surface” to calculate connectivity as the impedances of pixels relative to the minimum and maximum impedances of the landscape (Marulli & Mallarach, 2005). Resistance-based metrics have proven to be useful for calculating cost-corridors for use in conservation and landscape planning (Dickson et al., 2017). However, resistance-based metrics are not ideal for measurements of patch or landscape-level connectivity, particularly because they do not incorporate patch area.

Functional connectivity metrics can also be broken down into those that measure “landscape-level” and “patch-level” connectivity. A landscape-level connectivity metric is one that provides some estimate of connectivity of an entire landscape or polygon. Examples include the IIC, PC index, and ECA. A patch-level connectivity metric is one that quantifies how connected an individual landscape patch is within a landscape, generally with reference to the arrangement of the resource mosaic around the patch. Examples include Node betweenness centrality, Incidence Function Measure, and Flux (Albert et al., 2017; Bunn et al., 2000; Freeman, 1978; Hanski, 1994; Moilanen & Nieminen, 2002; D. Urban & Keitt, 2001). Both landscape and patch-level metrics are important for different analytical questions, and it follows that a well-designed metric should include extensions for both landscape and patch-level metrics. If we consider a landscape to be an assembly of patches, then landscapes with many highly functionally connected individual patches should have correspondingly high functional connectivity.

Keeley et al (2021) describes a decision tree for selecting the appropriate functional connectivity metric for specific analytical situations, however, multiple metrics can be used in each situation. The need for a metric generalizable to both patches and landscapes that also incorporates all elements of landscape connectivity (that is, Noss, Merriam, and Hanski connectivity) is evident. Of the metrics highlighted, the

PC index and ECA are two metrics that incorporate structural connectivity and may optionally incorporate functional connectivity. Here, we describe the Sinuous Connection Reduction (SCR) index, a functional connectivity metric based on the PC index and ECA, that may be used to assess the level of species-specific functional connectivity for an organism with a defined home-range and may be estimated at either the patch or landscape-level. The SCR index is developed from elements of resistance based metrics, the PC index, and simple structural connectivity metrics defined by Moilanen and Nieminen (Moilanen & Nieminen, 2002).

Methods

The SCR index was developed by modifying the PC index and ECA to retain their use of structural connectivity, while also integrating features of functional connectivity metrics through resistance based, least-cost-path modeling. The philosophy and mathematical formulation of the SCR index, including its modifications from the PC index and ECA, are described. We then evaluate the SCR index in comparison to the PC index and ECA using white-tailed deer (*Odocoileus virginianus*) as a case-study. We hypothesize that a more accurate functional connectivity metric will better fit the population density, i.e., population success, of white-tailed deer. The fit of the three metrics is compared using panel, spatial panel, and geographically weighted regression models. Biases of each metric are assessed by comparing how polygon size and boundaries influence each metric, such that the size and boundary location of a polygons should not influence the value for each metric.

Probability of Connectivity Index and Equivalent Connected Area

The SCR index is a modification of the probability of connectivity (PC) index, defined by Saura and Pascual-Hortal (2007). The PC index is a structural connectivity metric and is often modified to incorporate organism-specific dispersal parameters, but has several notable limitations (Saura et al., 2011). PC is formally written as:

(Eq. 1)

$$PC = \frac{\sum_{i=1}^n \sum_{j=1}^n a_i a_j p_{ij}^*}{A_L^2}$$

where a_i and a_j are the areas of habitat patches i and j within a landscape with a total area A_L . p_{ij} refers to the product probability (as a negative exponential function of interpatch distance) of a path between patches i and j :

(Eq. 2)

$$p_{ij} = e^{-\theta d_{ij}}$$

where θ is a species-specific constant that defines the rate of decay and d_{ij} is the distance between patches i and j . Meanwhile, p_{ij}^* is calculated as the maximum probability path by adding probability paths from i to j through all possible nodes. The PC index has the benefit of being bounded by zero and one, making it comparable to other metrics. However, the PC index is limited in that it has a tendency to return very low values if habitat patches are relatively small, and the total landscape area used is often arbitrary (Neel, 2008; Saura et al., 2011). An alternative metric, the equivalent connected area (ECA) addresses these concerns, but sacrifices the bounded minimums and maximums of the PC index (Saura et al., 2011). ECA is written formally as:

$$(Eq. 3) ECA = \sqrt{\sum_{i=1}^n \sum_{j=1}^n a_i a_j p_{ij}^*}$$

where all parameters are equivalent to that of the PC index.

The Sinuous Connection Reduction index

The SCR index operates under the assumptions of buffer-based connectivity metrics, specifically, an organism will move throughout its home range with little effect of distance (Moilanen & Nieminen, 2002). Instead, SCR aims to approximate individual-level organism movement decisions and dynamics by incorporating the irregularity of paths traveled in search of resources at new habitat patches, rather than for distance (Bennett & Tang, 2006). This approach also allows non-reachable yet adjacent habitat patches to be removed from the connectivity calculation. The SCR index also has the added benefit that it can be calculated at the scale of a single patch or entire landscape. The patch-level version of the index is written as:

(Eq. 4)

$$SCR_{patch} = \frac{a_i + \sum_{j=1}^n s_{ij}^* a_j}{A_{h_i}}$$

where a_i is the area of focal patch i and a_j is the area of patch j , located within a buffer of distance h from focal patch i . A_{h_i} is the area of the buffer around patch i , with a buffer distance typically set to be equivalent to a species-specific home range, h . Given that focal patch i is not likely to be circular, we to use h_i to represent distance in the place of the radius of a buffer. s_{ij}^* is the reciprocal of the sinuosity of the least-cost path between patches i and j , written as:

(Eq. 5)

$$s_{ij} = \frac{e_{ij}}{d_{ij}}$$

Where e_{ij} is the Euclidean distance between nodes i and j , and d_{ij} is the distance of the least-cost path between nodes i and j . Meanwhile, s_{ij}^* indicates that if there is no least-cost path between nodes i and j

, s_{ij}^* will equal zero, rather than being undefined. The landscape-level version of this index is expanded to:

(Eq. 6)

$$SCR_{landscape} = \frac{\sum_{i=1}^{n_i} a_i + \sum_{j=1}^{n_j} s_{ij}^* a_j}{n_i A_L}$$

Where n_i is the number of i patches within the landscape L (with area A_L) and n_j is the number of j patches within the species-specific home range. All other parameters are the same as the patch-level calculation.

White-tailed deer connectivity

White-tailed deer movement behavior was used to compare the performance of the SCR index to the PC index and ECA at the landscape level. White-tailed deer are a species of ungulates with a geographic range throughout temperate and north tropic zones of the western hemisphere (Rooney, 2001). White-tailed deer populations have been a concern among conservationists since at least the early 20th century, and are currently a concern among disease ecologists, forest managers, and landscape planners (Bourg et al., 2017; Burton et al., 2021; Diuk-Wasser et al., 2021; Leopold, 1943; Leopold et al., 1947; Nobert et al., 2016; Schmit et al., 2020; VanAcker et al., 2019, 2023). The response of white-tailed deer to the fragmentation of landscapes in ecotones remains an important area of study, particularly due to the role of white-tailed deer in the spread of tick-borne diseases (Diuk-Wasser et al., 2021; Kilheffer & Underwood, 2018). New York State (NYS) is a state in the northeastern United States with diverse geography resulting in a heterogenous distribution of white-tailed deer density. In particular, the Adirondack mountain range is an area of high elevation where harsh winter conditions force deer to congregate in lower elevation areas, resulting in lower deer-density (Hinton et al., 2022). Conversely, white-tailed deer populations in NYS often infiltrate highly urban areas, including New York City (VanAcker et al., 2023). Here, we estimate white-tailed deer functional connectivity in NYS to compare the SCR index to both the PC index and ECA.

Forest patch identification

White-tailed deer connectivity in NYS was estimated using the patch-level calculation of the SCR index (Eq. 4), and landscape-level calculation of the SCR index (Eq. 6), PC index (Eq. 1) and ECA (Eq. 3) using the boundaries of the Department of Environmental Conservation's (DEC) Wildlife Management Units (WMUs). Land cover classifications for each WMU in the form of raster data were obtained from the National Land Cover Database (2019) Land Cover Dataset at 30-meter resolution using the 'FedData' package in R version 4.2.2. (Bocinsky, 2020; Dewitz, 2021; R Core Team, 2022). Land cover classes of "deciduous forest," "evergreen forest", and "mixed forest" were recategorized as a single forest class to identify forested areas white-tailed deer may use as resource patches. Individual forest patches were then identified using the *l* and *s* *metrics* package in R using rook's adjacency rules (Hesselbarth et al., 2019). Forest patch analysis of recategorized forests identified 635,129 disjointed forest patches in NYS, 365,458 of which were either one 30m or two 30m raster cells. Forest patches were then

removed from analysis to decrease computation time and remove small patches white-tailed deer would be unlikely use as their predominant patch under the following logic: First, forest patches with an area equivalent to two or fewer 30m raster cells were excluded from analysis. Second, the remaining forest patches were separated into two groups: those with an area greater than the mean of all patches, and those with an area less than or equal to the mean of all patches. A random five-percent subset of the patches with an area less than or equal to the patch mean was then taken and rejoined to the patches with an area greater than the patch mean. Rejoining the forest patches with area less than or equal to the patch mean was done to avoid removing the potential effects small forest patches may have on landscape connectivity. The resulting set of 66,295 forest patches, covering 6,507,539 hectares were then considered as nodes for use in least-cost path modeling. A calculation using a single WMU (4R) was performed without removing any disjointed forest patches to ensure the subset of small forest patches did not dramatically influence connectivity metric results.

Resistance-raster data

Least-cost paths between focal forest patches and adjacent forest patches were estimated by calculating weighted resistance values at 30-meter resolution from parameters previously used in the literature to represent resistance to white-tailed deer movement (Girardet et al., 2015; Gurrutxaga et al., 2011; VanAcker et al., 2019). Parameter values from the literature were matched and averaged to generate final parameter values for use in the resistance raster. Land cover data was gathered from the National Land Cover Database (NLCD) 2019 Land Cover Dataset at 30-meter resolution (Jon Dewitz, 2024). NYS roadways were gathered as vector data from the 2020 NYS Roadway Inventory System Data via NYS ArcGIS Clearinghouse. Shapefiles for alpine regions in NYS were gathered from the Environmental Protection Agency’s Ecoregion shapefiles. Roadway and alpine region vector data were then resampled to raster data at 30-meter resolution to match the NLCD 2019 Land Cover Dataset. Resistance values were then summed for each cell among the land cover, roadway, and alpine region data to generate final resistance values. Resistance raster values, calculations and data sources are shown in Table 1. All operations on raster data were performed using the “terra” package in R (Hijmans, 2023).

Table 1: Resistance values and data sources for resistance raster used in least-cost path modeling.

Data source	Averaged Values		Gurrutxaga et al., 2011		Girardet et al., 2015		VanAcker et al., 2019	
National Land Cover Database (2019) Land Cover Dataset	Forest	1	Forest Edges	1	Forest	1	Forest	1
	Cropland	35	Agroforestry	15	Cultivated Fields	60		
	Wetland	100	Pastures	30				
			Water Bodies	100	Wetland and Water Bodies	100	Water	100
	Open Water ^a	1000						
	Low/Open Developed	27	Bushes	5	Forest Meadow	1 30	Grassland/shrub	1
2020 NYS Roadway Inventory System Data	Medium Developed	100					Paved surfaces	100
	High Developed	1000	Urban Areas	1000	Built Area	1000	Paved surfaces	100
							Buildings	1000
Environmental Protection Agency New York Ecoregions	Minor Roads	100			Minor Roads	100	Paved surfaces	100
	Highways	533			National Roads Highways and Fenced Roads	300 1000	Roads/railroads	300
	Non-alpine Elevation ^b	1						
	Alpine Elevation ^b	1000						

a - Open Water is distinguished from Water Bodies and Wetland in the literature and is self assigned.

b - Self-assigned designations based on personal communication with Jeremy Hurst.

Computation of forest metrics

The PC index, ECA and the landscape and patch-level SCR indices were calculated using parameters to estimate white-tailed deer movement behavior. Within $p_{ij}^* = e^{-\theta d_{ij}}$, θ was parameterized such that a distance of 1,675 meters (the chosen distance to represent the home-range of white tailed deer) returned a probability of 0.05 (Bunn et al., 2000; Williams et al., 2012). Similarly, focal patches and adjacent patch pairs used in the SCR index were assigned using a buffer distance of 1,675 meters. Examples of patch-level calculations of the SCR index taken are shown in Fig. 1 to demonstrate the behavior and concept of the metric. Patch areas and distances between i and j patches were calculated using the “sf” package in R (Pebesma, 2018). A network of nodes and edges for use in the PC index and ECA metric was built from the set of forest patch nodes for each WMU using the “igraph” package in R (Csárdi et al., 2023). Least-cost-paths between adjacency pairs were created calculated from the resistance raster using the ‘leastcostpath’ package in R (Lewis, 2023). Calculations of each metric were also performed on WMUs with borders extended to a buffer distance of 1,675 meters to determine each metrics susceptibility to edge effects. All calculations were performed using the University at Buffalo’s High Performance Computing Cluster.

Statistical Analysis

The utility of each of the PC index, ECA, and landscape-level SCR index were compared by assessing species-specific prediction, sensitivity to edge effects, and sensitivity to overall landscape size. Species-specific prediction utility was assessed by comparing metrics to counts of white-tailed deer take per hectare by hunters in NYS for each WMU from 1988 to 2021. Deer take per hectare was used as a proxy for while-tailed deer density and was provided by DEC. Using deer take per hectare as a proxy for white-

tailed deer density introduces several biases, namely through the introduction of hunting frequency and laws, rather than pure estimates of deer density. Despite the added bias, deer take per hectare (henceforth, deer per hectare) is commonly used by DEC as an estimate for a deer density throughout NYS. Each metric was compared to deer per hectare using a statistical modeling procedure, where a better fitting model is assumed to be a better indicator of functional connectivity. The statistical modeling utilized panel, spatial panel, and geographically weighted regression (GWR) models under the following procedure: Panel models were built using log-transformed counts of deer per hectare as dependent variables, metrics included as a fixed-effects independent variables, and WMUs included as a random-effect. The residuals of the panel models were then tested for residual spatial and serial autocorrelation via the Moran's I and Durbin-Watson tests, respectively ($\alpha = 0.05$) (Durbin & Watson, 1950; Moran, 1950). Moran's I tests were performed for each year and each metric for a total of 102 tests. P-values were adjusted using the Bonferroni-Holm correction to account for multiple-testing, and statistical significance was then assessed using an α of 0.05 (Holm, 1979). If residual spatial autocorrelation was detected, spatial panel models were used. If serial autocorrelation was detected, serially correlated remainder errors were accounted for in the spatial panel model. Spatial panel models were built using the same model formula as a-spatial panel models with the addition of a spatial lag parameter. A-spatial panel models, spatial panel models, and Moran's I and Durbin-Watson tests were calculated using the packages, "plm", "splm", and "spdep" in R (Bivand, 2022; Bivand et al., 2021; Millo, 2017; Millo & Piras, 2012). Metric performance was then assessed by comparing Akaike information criterion (AIC) for the spatial panel models of each metric.

Given the ecological heterogeneity of NYS, GWR models were built to determine if the relationship between each metric and deer per hectare varied over space. Centroids of WMUs were used as points in GWR models, and separate GWR models were built for each year of data. GWR models were built using non-adaptive bandwidths for kernel weighting functions and were calculated for each year of data. Model formulas included the log transformation of deer per hectare as a dependent variable and metric as an independent variable. Average β parameters for each year and each WMU were calculated. GWR models were built using the "spgwr" package in R (Bivand & Yu, 2022).

Assessing metric sensitivity to edge effects was performed by comparing metric values between WMUs and WMUs with buffered edges using the Kruskal-Wallis rank sum test ($\alpha = 0.05$). Calculating sensitivity to landscape size was performed by calculating linear models and generalized additive models (GAMs) relating WMU size to the value of each metric. The adjusted R^2 value from each was used to estimate the sensitivity of each metric to landscape size. Linear models and GAMs were built in R using base R and the "mgcv" package, respectively (R Core Team, 2022; Wood, 2011). These methods operated under the assumption that if a metric is influenced by the size of the landscape, the models will explain more of the variance in landscape area. The relationship of each metric to landscape size was also estimated visually by plotting linear models and GAM smoothing functions using the "ggplot" package in R (Wickham, 2016).

Results

PC index, ECA, and SCR index calculations

The patch-level SCR index was successfully calculated for the subset of 66,295 forest patches in NYS. A map and distribution of the SCR index is shown in Fig. 2. The PC index, ECA, and SCR index were successfully calculated for all 92 WMUs in NYS. SCR index values were also calculated on a full set and a subset of forest patches within WMU 4R. Within WMU 4R, calculations using both the full set of 2,376 forest patches and the subset of 81 forest patches both resulted in SCR values of 0.322. Landscape-level values for the PC index ranged from 3.06×10^{-9} to 0.475 (mean of 0.090) for unbuffered WMUs and 3.62×10^{-6} to 0.444 (mean of 0.049) for buffered WMUs. Values for ECA ranged from 1.49 to 498,836.6 (mean 36,209.23) for unbuffered WMUs and 569.83 to 239,911.8 (mean 24,382.25). Values for the SCR index ranged from 7.88×10^{-4} to 0.833 (mean 0.0935) for unbuffered WMUs and 6.33×10^{-4} to 0.737 (mean 0.0778) for buffered WMUs. The distribution of each metric using unbuffered and buffered WMUs are shown in Fig. 3. Choropleth map displaying the values for each metric along with a raster of forests classified by the NLCD 2019 Land Cover Dataset are shown in Fig. 4.

Statistical analysis comparing metrics to white-tailed deer density

All three aspatial panel models indicated a statistically significant and negative relationship between each metric and deer density. The ECA model explained the most variation in deer density ($R^2 = 0.243$) followed by SCR ($R^2 = 0.173$), and PC index ($R^2 = 0.096$). Panel models assessing the relationship between each connectivity metric and log transformed deer per hectare are shown in Table 2. Durbin-Watson tests detected residual serial autocorrelation for the SCR index (DW = 0.100, $p = < 0.0001$), PC index (DW = 0.092, $p = < 0.0001$), and ECA (DW = 0.115, $p = < 0.0001$). Similarly, Moran's I tests detected residual spatial autocorrelation for all three models in 97 out of 102 years examined. The results of each Moran's I test are shown in Supplemental Fig. 1. Spatial panel models were built for each connectivity metric following residual serial and spatial autocorrelation in the aspatial panel models. All three spatial panel models indicated a statistically significant negative relationship between each metric and deer density. Model results for all three spatial panel models are shown in Table 3. The model for ECA was the best fitting model (Log-likelihood = 982.85), followed by SCR (Log-likelihood = 979.42) and PC index (Log-likelihood = 975.59). GWR models indicated that the relationship between each metric and deer per hectare varied with space. Choropleth maps of average β coefficients for each metric are shown in Fig. 5.

Table 2

Aspatial panel models comparing Sinuous Connection Reduction index, Probability of Connectivity index and Equivalent Connected Area metrics to white-tailed deer take per hectare, as a proxy for white-tailed deer density. Model fit is assessed via R^2 values. Year of white-tailed deer take is included as an additional independent variable.

Model	Coefficient	Estimate	Std. Error	Z-value	P-value
Sinuous Connection Reduction (SCR) ($R^2 = 0.173$)					
	Intercept	-3.93	0.049	-80.72	< 0.0001
	SCR	-1.90	0.076	-25.12	< 0.0001
	Year	0.001	0.002	0.560	0.575
Probability of Connectivity (PC) ($R^2 = 0.096$)					
	Intercept	-3.92	0.049	-79.22	< 0.0001
	PC	-2.14	0.120	-17.90	< 0.0001
	Year	0.001	0.002	0.560	0.575
Equivalent Connected Area (ECA) ($R^2 = 0.243$)					
	Intercept	-3.89	0.049	-79.84	< 0.0001
	ECA	-6.06E-06	1.95E-07	-31.14	< 0.0001
	Year	0.001	0.002	0.560	0.575

Table 3

Spatial panel models comparing Sinuous Connection Reduction index, Probability of Connectivity index and Equivalent Connected Area metrics to white-tailed deer take per hectare, as a proxy for white-tailed deer density. Model fit is assessed via log-likelihood values. Year of white-tailed deer take is included as an additional independent variable.

Model	Coefficient	Estimate	Std. Error	t-value	P-value
Sinuous Connection Reduction (SCR) (Log-likelihood = 979.61)					
	Intercept	-1.89	0.080	-23.53	< 0.0001
	SCR	-1.18	0.354	-3.35	0.0001
	Year	0.00	0.002	0.60	0.55
Probability of Connectivity (PC) (Log-likelihood = 975.77)					
	Intercept	-1.92	0.092	-20.93	< 0.0001
	PC	-0.93	0.559	-1.67	0.095
	Year	0.001	0.002	0.59	0.553
Equivalent Connected Area (ECA) (Log-likelihood = 983.03)					
	Intercept	-1.87	0.079	-23.62	< 0.0001
	ECA	-4.03E-06	9.20E-07	-4.38	< 0.0001
	Year	0.001	0.002	0.61	0.542

Sensitivity to edge effects and polygon area

Kruskal-Wallis rank sum tests comparing each metric using WMUs and buffered WMUs were statistically significant for both the PC index ($\chi^2 = 30.851$, $p < 0.0001$) and ECA ($\chi^2 = 16.278$, $p < 0.0001$), while the WMUs and buffered WMUs were not statistically significant for the SCR index ($\chi^2 = 1.101$, $p = 0.294$.) Linear models and GAMs indicated a statistically significant relationship between the size of a WMU and the value for each of the PC index, SCR index and ECA. Using linear models, the PC index had the lowest variability explained ($R^2 = 0.036$), followed by the SCR index ($R^2 = 0.083$) and ECA ($R^2 = 0.639$). Results from linear models are shown in Table 4. Variance explained using GAMs followed a similar trend; the PC index had the lowest variability explained ($R^2 = 0.163$), followed by the SCR ($R^2 = 0.197$) and ECA ($R^2 = 0.836$). Linear models and GAMs are displayed in Supplemental Fig. 2.

Table 4
Linear models assessing the relationship between polygon size and the connectivity value for the Sinuous Connection Reduction index, Probability of Connectivity index, and Equivalent Connected Area. Model fit is assessed via R^2 values.

Model	Coefficient	Estimate	Std. Error	t-value	P-value
Sinuous Connection Reduction (SCR) ($R^2 = 0.083$)					
	Intercept	0.037	0.005	8.08	< 0.0001
	SCR	4.26E-07	2.58E-08	16.49	< 0.0001
Probability of Connectivity (PC) ($R^2 = 0.036$)					
	Intercept	0.067	0.003	21.51	< 0.0001
	PC	1.85E-07	1.75E-08	10.58	< 0.0001
Equivalent Connected Area (ECA) ($R^2 = 0.639$)					
	Intercept	-23850	1078	-22.12	< 0.0001
	ECA	0.440	0.006	73.14	< 0.0001

Discussion

Assessing a novel connectivity metric

Conceptually, Merriam, Hanski, and Noss connectivity are simplifications of a complex ecological phenomenon, while the metrics used to quantify them are greater simplifications still. Inevitably, each layer of simplification introduces unintended biases and information loss in exchange for parsimony. The goal of any metric should be to reduce bias and best approximate the system in question. Here, we examine the utility and biases of the SCR index and its precursors by assessing:

1. The properties of each metric, including potential biases that may arise during their use.
2. Whether each metric approximates Merriam, Hanski, and/or Noss connectivity.
3. How the behavior of each metric can be used to inform white-tailed deer ecology.
4. The use cases and future direction of the SCR index.

Properties of calculated landscape connectivity metrics

The SCR index is a functional connectivity metric developed from the PC index, ECA, and associated concepts described in Saura and Pascual-Hortal (2007) and Saura et al. (2011). Saura and Pascual-Hortal (2007) outline 13 desirable properties of a landscape connectivity metric; the PC index holds all 13 of these desirable properties, while the ECA holds 12 of the 13. The property lost by the ECA is described in Saura et al., (2011); the ECA can take any value and therefore does not have a predefined

and bounded range of variation. We define three additional properties a landscape connectivity metric should possess: both landscape and patch-level extensions of the metric, and resilience to both boundary-effects and changes in overall landscape area. The SCR index, PC index, and ECA area evaluated against the original 13 desirable properties presented in Saura and Pascual-Hortal (2007) and the three additional properties defined in this paper, in Table 5.

The SCR index holds 11 of the 13 properties originally described in Saura and Pascual-Hortal (2007). The two properties lost when calculating the SCR index are the ability to be computed on both vector and raster data, and a lower connectivity result when the distance between patches decrease. The formula for the SCR index is similar to the PC index, and the changes made to the formula result in the loss of these properties. The most notable limitation of the SCR index is represented in the inability to be computed on both vector and raster data. The SCR index, like all resistance-based metrics, requires raster data. The PC index is versatile in this respect because it can be calculated using a simply distance-decay function and the orientation of resource patches as polygon data. If desired, the PC index can utilize raster-based least-cost paths for distance measures, rather than Euclidean distance. The SCR index loses the property of decreasing connectivity when distance decreases due to its use of a buffer-based home-range. The use of this property is reflective of a different conceptualization of connectivity. While the PC index uses a distance decay function to calculate probabilities throughout the entire network of a landscape mosaic, the SCR index assess the connectivity of a focal patch to first-order adjacent patches within the home-range buffer. Incorporating home range partially achieves the goal of increasing distance resulting in lower connectivity; patches outside the home-range will not contribute to the connectivity of the focal patch. More importantly, conceptualizing connectivity as first-order adjacent connections approximates an individual organism's decisions at small scales. Rather than calculating connectivity as the likelihood an organism moves between a focal patch to any other patch within a landscape, connectivity can be conceptualized hierarchically as the accumulation of movement decisions between a focal patch and first-order adjacent patches. Dynamic models built to approximate animal movement are often built to incorporate multiple spatial scales, rather than using a network of between patch distances (Bennett & Tang, 2006; Tang & Bennett, 2010)

Boundary effects occur when spatially explicit calculations are impacted by a boundary or delineation. The nearest-neighbor statistic is a common example of a statistic impacted by adjacency to a boundary; the nearest-neighbor of a point may be across a boundary, resulting in its exclusion from analysis (Rogerson, 2021). To avoid bias in studies of natural phenomena, boundaries should be selected to best approximate the natural system in question (Jackson et al., 2006). A landscape connectivity metric quantifying Merriam connectivity should approximate the movement of an organism regardless of human-defined and non-phenomenon generating boundaries. White-tailed deer functional connectivity should involve capturing the movement potential of white-tailed deer to all forest patches within their home range including patches beyond and along artificial and geopolitical boundaries. Kruskal-Wallis tests resulted in a statistically significant difference in the distribution of buffered and unbuffered WMUs for both the PC index and ECA, indicating these metrics fail to capture the movement potential of white-tailed to all forest patches available to them. Conversely, there is no statistically significant difference

between buffered and unbuffered WMUs when calculating the SCR index, indicating a resilience to potential bias. A likely explanation for the difference in susceptibilities of these metrics lies in their calculation. Both the PC index and ECA calculate connectivity by calculating paths between each patch and all other patches in the landscape, where the number of comparisons equals $\sum_{i=n-1}^1 i$. Adding additional area to a landscape increases the number of calculations required, and the increase is greater for larger landscapes. For example, when calculating the PC index for the WMU with the fewest number of patches, the number of comparisons increased from 190 to 1,128 (+ 938) between the unbuffered and buffered WMUs. When the PC index was calculated for the WMU with the highest number of patches, the number of comparisons increased from 5,516,181 to 6,677,685 (+ 1,161,504) between the unbuffered and buffered WMUs. The landscape-level SCR index calculates paths from all patches to all patches within the home range of the organism examined, greatly reducing the number of computations. As a result, the movement potential does not impact patches in the center of a landscape when boundaries are changed.

Resilience to boundary effects can also be seen as resilience to the modifiable areal unit problem (MAUP). The MAUP is the geographic extension of the ecological fallacy, whereby changing areal units (polygons) used for aggregation results in bias (Buzzelli, 2020; Gehlke & Biehl, 1934; Robinson, 1950). Efforts in conservation biogeography have involved categorizing and recategorizing the terrestrial ecology of Earth into distinct ecoregions, despite the continuous nature of ecology (Olson et al., 2001; Udvardy, 1975). New York State's WMUs also aim to aggregate ecology into areal units, however, both efforts suffer from the potential bias of the MAUP. The process of aggregating ecological systems to artificial geopolitical or semi-geopolitical boundaries simplifies the continuous nature of these systems, impacting visualizations, statistical results, and the understanding of ecological phenomena (Jelinski & Wu, 1996; O'Connor et al., 2024; Openshaw, 1984; Openshaw & Taylor, 1979). Despite bias from the MAUP, areal-unit categorizations continue to be used for their logistical and geopolitical utility. Like the areal-units themselves, landscape-level connectivity metrics should attempt quantify connectivity while considering the underlying continuous and dynamic ecological systems they represent, making a point to reduce bias from such categorizations.

A second desirable property of a connectivity metric is being unaffected when the area of a landscape changes. Feasibly, the quantitative estimate of connectivity should ignore overall landscape size by instead incorporating the density of resource patches. As a heuristic, all landscapes should have similar values for connectivity if they have similar relative proportion of resource patches within them, regardless of the overall landscape size. Of the three metrics, the size of the landscape explained the smallest amount of variability in values of the PC index, followed by the SCR index and ECA. Of the three metrics, ECA had the largest proportion of the variability explained by the size of the landscape. These results were expected, given the formulae for each metric. Both the PC and SCR indices are calculated relative to the landscape size by including the area of the landscape in the denominator, while the ECA does not. By not incorporating landscape size, the ECA formula introduces a bias caused by using absolute dispersion over relative dispersion (McGrew & Monroe, 2000; Rogerson, 2015). This bias is

depicted in Fig. 6, where the PC index and ECA are calculated using forest patches in Central Park of Manhattan, New York City. The calculation is performed using the landscape of Central Park, as well as the landscape of Manhattan without adding additional forest patches in the calculation. The resulting SCR and PC indices for both landscapes track with the relative dispersion of forest patches; as the landscape increases while the forest patches used stay the same, the SCR PC indices decrease. Conversely, ECA remains the same for both calculations due to its use of absolute dispersion.

We also note that a landscape metric should possess both patch and landscape-level extensions of a metric. The ability to calculate a patch and landscape-level metric provides increased utility as it can be used in multiple analytical situations. Further, if the metric is also bounded by a pre-defined range, both versions of the calculation are immediately comparable. This property allows for a researcher to assess which patches within a landscape are contributing to the overall quantification of the connectivity of a landscape, and fits with the scale-dependent nature of landscape ecology (Jelinski & Wu, 1996; Wiens, 1989; Wiens & Milne, 1989). The landscape-level extension of the SCR index approximates this phenomenon by aggregating the results of patch-level metrics within a landscape to quantify the landscape's overall connectivity. Using both patch level and landscape-level calculations also allows the landscape to be analyzed hierarchically to examine emergent properties in landscape ecology (Li & Wu, 2004). For example, individual patches can be examined in reference to their connectivity to adjacent patches, groups of patches within a landscape can be examined to identify connected corridors, and the entire landscape can be examined and compared to other nearby landscapes. Both the patch and landscape-level calculation of the SCR index match reasonably well with the continuous distribution of large and clustered forest patches in NYS (Figs. 2 and 4). Though the PC index and ECA also approximate the distribution of forest patches in NYS at the landscape-level, it is not immediately obvious if this relationship matches at smaller scales.

Assessing Merriam, Hanski, and Noss connectivity

The SCR index, PC index, and ECA fall into categories of connectivity metrics that incorporate both structural and functional connectivity. All three metrics clearly incorporate Noss connectivity; the SCR index uses a buffer-based metric and assigns edges and nodes as a graph within the buffer, while the PC index and ECA operate by creating a graph for all nodes in the landscape. Less clear are the levels at which each metric incorporates Merriam and Hanski connectivity. Conversely, each metric fails to incorporate Hanski connectivity, as reproductive success is not considered or parameterized in the metric calculation process. Fahrig et al. (2021) depict Hanski connectivity as using landscape structure with the goal of assessing population success. Under this formulation, population success is seen as the outcome of a highly connected landscape. In keeping with Fahrig et al. (2021), this study chose to model population success as an outcome, i.e., the dependent variable, by using deer density as a measure of population success. Meanwhile, each metric quantifies Merriam connectivity and is concerned with the potential movement of an organism between patches within the landscape. The SCR index incorporates Merriam connectivity the most directly by requiring the use of least-cost paths based on resistance to animal movement. Though the PC index and ECA can also incorporate least-cost paths, their calculation

becomes computationally burdensome given their need to calculate paths throughout the entire network. When calculating the PC index and ECA using only distance decay and polygon orientation, Merriam connectivity is only incorporated as the parameterized distance-decay function, rather than incorporating other movement-specific decisions and rules. By only incorporating one parameter for movement, the PC index and ECA are primarily structural connectivity metrics.

Implications for understanding white-tailed deer functional connectivity

The habitat generalist behavior of white-tailed deer makes modeling their functional connectivity difficult. Given the massive geographic range of white-tailed deer, variation in forest arrangement and the resulting estimations of white-tailed deer movement potential may not accurately describe the variability of white-tailed deer populations. Figure 5 best illustrates this, as GWR models for all forest metrics indicate directionally opposite β coefficients in different regions of NYS. One potentially confounding variable is the impact of elevation and snowpack on white-tailed deer population (Hinton et al., 2022). The Adirondack Mountains are a mountain range in northeastern NYS (Fig. 4D) with generally low deer per hectare (Fig. 5D). Figures 4A, 4B, and 4C display high values for all forest metrics in this same region despite high values for forest connectivity. Conversely, regions where the relationship between forest connectivity metrics and deer per hectare are positive seem to lie where forests are more fragmented. The regionally specific relationship between forest connectivity and white-tailed deer density could point to different mechanisms defining white-tailed deer functional connectivity: Navigation through decision making processes in fragmented landscapes presumably becomes more important when a larger proportion of the overall landscape is not made up of resource patches. Conversely, when nearly all the landscape within the home-range of a white-tailed deer can be considered a resource patch, the population of white-tailed deer may instead be modulated by exogenous factors (e.g., weather patterns, risk of predation) rather than forest arrangement.

Framing these results as separate mechanisms may partially agree with aspects of deer behavior in relation to urbanization. Some evidence indicates the urbanization of key deer (a subspecies of white-tailed deer) decreases flight distance and increases group size, suggesting urbanized deer have a decreased fear response and utilize human resources more effectively (Harveson et al., 2007; Peterson et al., 2005). However, a recent study by Maurer et al., (2022) indicates intensity of site use increased away from human developments, representing human avoidance behaviors. Additionally, deer detection rate exponentially increased with distance from a development if deer were seen on a human constructed trail. Detection of deer more frequently on human constructed trails further from human developments could represent an aspect of deer landscape usage that is represented by the GWR coefficients in Fig. 5. When examining deer connectivity in less connected regions, deer functional connectivity increases with distance from human developments. Trails could be a useful proxy for the relationship between functional connectivity and distance, as hiking trails likely exist outside of urban developments. In this scenario, the relationship between connectivity and deer density (via deer take) is

positive. When considering regions farthest away from human settlements, it is possible that functional connectivity becomes less relevant.

Use cases, benefits, and future direction of Sinuous Connection Reduction:

Although white-tailed deer provide a well-known and complex model organism to examine the utility of the SCR index and associated metrics, each metric failed to capture some of the dynamics of white-tailed deer ecology in NYS. A functional landscape connectivity approach may be better fit to study habitat-specific organisms or white-tailed deer connectivity within smaller regions. With these limitations in mind, it appears the SCR index is at minimum comparable in accuracy to the PC index, and at best provides an alternative that is useful at patch and landscape scales. Further, the SCR index may be more computationally efficient than the PC index and ECA in areas with many forest patches. Calculating the SCR index on the buffered WMU with the highest number of forest patches took 27 minutes and 22 seconds on an Intel Xeon Gold 6330 2G, 28C/56T, 11.2GT/s, 42M Cache, Turbo, HT (205W) DDR4-2933 using 400 gigabytes of RAM and 24 cores in parallel. Comparatively, calculating the PC index using the same polygon and set of forest patches took just under 10 days, though the code used to calculate the PC index could be improved to increase efficiency. The most notable limitation of the SCR index is that it can only be calculated using data-intensive least-cost-path modeling, where the PC index and ECA only require landscape polygons and resource patch arrangements within the polygons. The PC index and ECA may also be calculated using least-cost-path modeling as a measure of between-patch distance, but computational efficiency becomes an issue for large landscapes.

The SCR index also holds the added benefit that it can be usefully applied to agent-based modeling (ABM) efforts, particularly those that attempt to model population inflows and outflows at disjointed patches. Crooks & Hailegiorgis, (2014) modeled behavior in humans using the scenario of the Dagahaley, Ifo, and Hagadera sites within the Dadaab refugee camp in Kenya. The three sites at Dadaab are geographically collinear and agents moved between first-order adjacent sites using a least-cost path algorithm. The movement of agents between first-order adjacent patches is easily captured in ABMs, as an agent's decision if and how to move to an adjacent patch can be assessed at each individual time step; an understanding of the total network is not necessary. The SCR index uses home-range to capture all first-order adjacent patches to the focal patch and captures the difficulty of movement using least-cost path modeling. Comparatively, the PC index and ECA capture $\sum_{i=n-1}^1 i$ comparisons for n patches, where adjacency is conceptually replaced by considering patches as "stepping-stones" and movement is guided by a distance decay function. This feature makes the PC index better suited for modeling networks rather than movement between adjacent patches. We posit the SCR index is better fit to incorporate into ABM methodologies, particularly data exploration, calibration, and validation.

The SCR metric and its application to white-tailed deer connectivity contain several limitations, namely the use of proxy data for white-tailed deer density, accuracy of parameters used for white-tailed deer least-cost path models, and the data-intensive requirements of resistance-based least-cost path

modeling. Our results indicate the SCR index is not to be used as a replacement to the PC index or ECA, however, it can be used in specific analytical situations with comparable results. The SCR index can be used to assess functional connectivity when an organism's home-range can be used to model first-order adjacency of resource patches. Using the SCR index for this reason may also be more parsimonious, accurate at capturing movement dynamics, computationally efficient, and reduce bias from boundary effects when studying a landscape with large numbers of disjointed patches. The SCR index should not be substituted for the PC index when analytical situations call for a complete understanding of the network of a landscape. However, we hope the use of the SCR index can provide a better understanding of landscape connectivity at multiple spatial scales in future ecological applications.

Declarations

Data availability:

All code and data used for this paper is publicly available at doi: 10.5281/zenodo.12522571. The code is presented in reproducible format and can be used to recreate all results including statistical analysis and figure generation.

Acknowledgements:

The authors would like to thank Jeremy Hurst at the New York State Department of Conservation for supplying white-tailed deer take data, and for providing modeling advice regarding white-tailed deer ecology.

References

1. Albert, C. H., Rayfield, B., Dumitru, M., & Gonzalez, A. (2017). Applying network theory to prioritize multispecies habitat networks that are robust to climate and land-use change. *Conservation Biology*, 31(6), 1383–1396. <https://doi.org/10.1111/cobi.12943>
2. Baudry, J., & Merriam, G. (1988). Connectivity and connectedness: Functional versus structural patterns in landscapes. *Connectivity in Landscape Ecology*, 29, 23–28.
3. Bennett, D. A., & Tang, W. (2006). Modelling adaptive, spatially aware, and mobile agents: Elk migration in Yellowstone. *International Journal of Geographical Information Science*, 20(9), 1039–1066. <https://doi.org/10.1080/13658810600830806>
4. Bivand, R. (2022). R Packages for Analyzing Spatial Data: A Comparative Case Study with Areal Data. *Geographical Analysis*, 54(3), 488–518. <https://doi.org/10.1111/gean.12319>
5. Bivand, R., Millo, G., & Piras, G. (2021). A Review of Software for Spatial Econometrics in R. *Mathematics*, 9(11), 1276. <https://doi.org/10.3390/math9111276>
6. Bivand, R., & Yu, D. (2022). *spgwr: Geographically Weighted Regression* (0.6-35) [R]. <https://CRAN.R-project.org/package=spgwr>

7. Bocinsky, R. K. (2020). *FedData: Functions to Automate Downloading Geospatial Data Available from Several Federated Data Sources* [Computer software]. <https://CRAN.R-project.org/package=FedData>
8. Bossart, J. L., & Pashley Prowell, D. (1998). Genetic estimates of population structure and gene flow: Limitations, lessons and new directions. *Trends in Ecology & Evolution*, 13(5), 202–206. [https://doi.org/10.1016/S0169-5347\(97\)01284-6](https://doi.org/10.1016/S0169-5347(97)01284-6)
9. Bourg, N. A., McShea, W. J., Herrmann, V., & Stewart, C. M. (2017). Interactive effects of deer exclusion and exotic plant removal on deciduous forest understory communities. *AoB PLANTS*, 9(5). <https://doi.org/10.1093/aobpla/plx046>
10. Bunn, A. G., Urban, D. L., & Keitt, T. H. (2000). Landscape connectivity: A conservation application of graph theory. *Journal of Environmental Management*, 59(4), 265–278. <https://doi.org/10.1006/jema.2000.0373>
11. Burton, J. I., Mladenoff, D. J., Forrester, J. A., & Clayton, M. K. (2021). Effects of forest canopy gaps on the ground-layer plant community depend on deer: Evidence from a controlled experiment. *Journal of Vegetation Science*, 32(1). <https://doi.org/10.1111/jvs.12969>
12. Buzzelli, M. (2020). Modifiable Areal Unit Problem. In *International Encyclopedia of Human Geography* (pp. 169–173). Elsevier. <https://doi.org/10.1016/B978-0-08-102295-5.10406-8>
13. Crooks, A. T., & Hailegiorgis, A. B. (2014). An agent-based modeling approach applied to the spread of cholera. *Environmental Modelling & Software*, 62, 164–177. <https://doi.org/10.1016/j.envsoft.2014.08.027>
14. Csárdi, G., Nepusz, T., Müller, K., Horvát, S., Traag, V., Zanini, F., & Noom, D. (2023). *igraph for R: R interface of the igraph library for graph theory and network analysis* (v1.5.0) [Computer software]. Zenodo. <https://doi.org/10.5281/ZENODO.7682609>
15. Dewitz, J. (2021). *National Land Cover Database (NLCD) 2019 Products* [dataset]. U.S. Geological Survey. <https://doi.org/10.5066/P9KZCM54>
16. Dickson, B. G., Albano, C. M., McRae, B. H., Anderson, J. J., Theobald, D. M., Zachmann, L. J., Sisk, T. D., & Dombek, M. P. (2017). Informing Strategic Efforts to Expand and Connect Protected Areas Using a Model of Ecological Flow, with Application to the Western United States: Mapping ecological flow to inform planning. *Conservation Letters*, 10(5), 564–571. <https://doi.org/10.1111/conl.12322>
17. Dieckmann, U., O'Hara, B., & Weisser, W. (1999). The evolutionary ecology of dispersal. *Trends in Ecology & Evolution*, 14(3), 88–90. [https://doi.org/10.1016/S0169-5347\(98\)01571-7](https://doi.org/10.1016/S0169-5347(98)01571-7)
18. Dijkstra, E. W. (1959). A note on two problems in connexion with graphs. *Numerische Mathematik*, 1(1), 269–271. <https://doi.org/10.1007/BF01386390>
19. Diuk-Wasser, M. A., VanAcker, M. C., & Fernandez, M. P. (2021). Impact of Land Use Changes and Habitat Fragmentation on the Eco-epidemiology of Tick-Borne Diseases. *Journal of Medical Entomology*, 58(4), 1546–1564. <https://doi.org/10.1093/jme/tjaa209>
20. Dunning, J. B., Danielson, B. J., & Pulliam, H. R. (1992). Ecological Processes That Affect Populations in Complex Landscapes. *Oikos*, 65(1), 169. <https://doi.org/10.2307/3544901>

21. Durbin, J., & Watson, G. S. (1950). Testing for Serial Correlation in Least Squares Regression: I. *Biometrika*, 37(3/4), 409. <https://doi.org/10.2307/2332391>
22. Fahrig, L., Arroyo-Rodríguez, V., Cazetta, E., Ford, A., Lancaster, J., & Ranius, T. (2021). Landscape Connectivity. In *The Routledge Handbook of Landscape Ecology* (1st ed., pp. 67–88). Routledge. <https://www.taylorfrancis.com/books/9780429399480>
23. Freeman, L. C. (1978). Centrality in social networks conceptual clarification. *Social Networks*, 1(3), 215–239. [https://doi.org/10.1016/0378-8733\(78\)90021-7](https://doi.org/10.1016/0378-8733(78)90021-7)
24. Gehlke, C. E., & Biehl, K. (1934). Certain Effects of Grouping upon the Size of the Correlation Coefficient in Census Tract Material. *Journal of the American Statistical Association*, 29(185A), 169–170. <https://doi.org/10.1080/01621459.1934.10506247>
25. Girardet, X., Conruyt-Rogeeon, G., & Foltête, J.-C. (2015). Does regional landscape connectivity influence the location of roe deer roadkill hotspots? *European Journal of Wildlife Research*, 61(5), 731–742. <https://doi.org/10.1007/s10344-015-0950-4>
26. Gurrutxaga, M., Rubio, L., & Saura, S. (2011). Key connectors in protected forest area networks and the impact of highways: A transnational case study from the Cantabrian Range to the Western Alps (SW Europe). *Landscape and Urban Planning*, 101(4), 310–320. <https://doi.org/10.1016/j.landurbplan.2011.02.036>
27. Hanski, I. (1994). A Practical Model of Metapopulation Dynamics. *The Journal of Animal Ecology*, 63(1), 151. <https://doi.org/10.2307/5591>
28. Harveson, P. M., Lopez, R. R., Collier, B. A., & Silvy, N. J. (2007). Impacts of urbanization on Florida Key deer behavior and population dynamics. *Biological Conservation*, 134(3), 321–331. <https://doi.org/10.1016/j.biocon.2006.07.022>
29. Hesselbarth, M. H. K., Sciaini, M., With, K. A., Wiegand, K., & Nowosad, J. (2019). *landscapemetrics*: An open-source R tool to calculate landscape metrics. *Ecography*, 42(10), 1648–1657. <https://doi.org/10.1111/ecog.04617>
30. Hijmans, R. J. (2023). *terra: Spatial Data Analysis* (R package version 1.7-29) [Computer software]. <https://CRAN.R-project.org/package=terra>
31. Hinton, J. W., Hurst, J. E., Kramer, D. W., Stickles, J. H., & Frair, J. L. (2022). A model-based estimate of winter distribution and abundance of white-tailed deer in the Adirondack Park. *PLOS ONE*, 17(8), e0273707. <https://doi.org/10.1371/journal.pone.0273707>
32. Holm, M. (1979). A simple sequentially rejective multiple test procedure. *The Scandinavian Journal of Statistics*, 6(2), 65–70.
33. Horskins, K., Mather, P. B., & Wilson, J. C. (2006). Corridors and connectivity: When use and function do not equate. *Landscape Ecology*, 21(5), 641–655. <https://doi.org/10.1007/s10980-005-5203-6>
34. Inglis, G., & Underwood, A. J. (1992). Comments on Some Designs Proposed for Experiments on the Biological Importance of Corridors. *Conservation Biology*, 6(4), 581–586. <https://doi.org/10.1046/j.1523-1739.1992.06040581.x>

35. Jackson, L., Levine, J., & Hilborn, E. (2006). A comparison of analysis units for associating Lyme disease with forest-edge habitat. *Community Ecology*, 7(2), 189–197.
<https://doi.org/10.1556/ComEc.7.2006.2.6>
36. Jelinski, D. E., & Wu, J. (1996). The modifiable areal unit problem and implications for landscape ecology. *Landscape Ecology*, 11(3), 129–140. <https://doi.org/10.1007/BF02447512>
37. Jon Dewitz. (2024). *National Land Cover Database (NLCD) 2019 Products (ver. 3.0, February 2024)* [dataset]. [object Object]. <https://doi.org/10.5066/P9KZCM54>
38. Keeley, A. T. H., Beier, P., & Jenness, J. S. (2021). Connectivity metrics for conservation planning and monitoring. *Biological Conservation*, 255, 109008. <https://doi.org/10.1016/j.biocon.2021.109008>
39. Kilheffer, C., & Underwood, H. B. (2018). Hierarchical patch delineation in fragmented landscapes. *Landscape Ecology*, 33(9), 1533–1541. <https://doi.org/10.1007/s10980-018-0679-z>
40. Leopold, A. (1943). Deer Irruptions. *Wisconsin Conservation Bulletin*, 8(8), 2–11.
41. Leopold, A., Sowls, L. K., & Spencer, D. L. (1947). A Survey of Over-Populated Deer Ranges in the United States. *The Journal of Wildlife Management*, 11(2), 162–177.
42. Levins, R. (1969). Some Demographic and Genetic Consequences of Environmental Heterogeneity for Biological Control. *Bulletin of the Entomological Society of America*, 15(3), 237–240.
<https://doi.org/10.1093/besa/15.3.237>
43. Lewis, J. (2023). *leastcostpath: Modelling Pathways and Movement Potential Within a Landscape* (2.0.11) [Computer software]. <https://github.com/josephlewis/leastcostpath>
44. Li, H., & Wu, J. (2004). Use and misuse of landscape indices. *Landscape Ecology*, 19(4), 389–399.
<https://doi.org/10.1023/B:LAND.0000030441.15628.d6>
45. Marulli, J., & Mallarach, J. (2005). A GIS methodology for assessing ecological connectivity: Application to the Barcelona Metropolitan Area. *Landscape and Urban Planning*, 71(2–4), 243–262.
[https://doi.org/10.1016/S0169-2046\(04\)00079-9](https://doi.org/10.1016/S0169-2046(04)00079-9)
46. Maurer, A. S., Cove, M. V., Siegal, O. M., & Lashley, M. A. (2022). Urbanization affects the behavior of a predator-free ungulate in protected lands. *Landscape and Urban Planning*, 222, 104391.
<https://doi.org/10.1016/j.landurbplan.2022.104391>
47. McGrew, J. C., & Monroe, C. B. (2000). *Introduction to statistical problem solving in geography*. McGraw-Hill.
48. McRae, B. H., Dickson, B. G., Keitt, T. H., & Shah, V. B. (2008). USING CIRCUIT THEORY TO MODEL CONNECTIVITY IN ECOLOGY, EVOLUTION, AND CONSERVATION. *Ecology*, 89(10), 2712–2724.
<https://doi.org/10.1890/07-1861.1>
49. Merriam, G. (1984). *Connectivity: A fundamental ecological characteristic of landscape pattern*. 5–15.
50. Metzger, J.-P., & Décamps, H. (1997). The structural connectivity threshold: An hypothesis in conservation biology at the landscape scale. *Acta Oecologica*, 18(1), 1–12.
[https://doi.org/10.1016/S1146-609X\(97\)80075-6](https://doi.org/10.1016/S1146-609X(97)80075-6)

51. Millo, G. (2017). Robust Standard Error Estimators for Panel Models: A Unifying Approach. *Journal of Statistical Software*, 82(3). <https://doi.org/10.18637/jss.v082.i03>
52. Millo, G., & Piras, G. (2012). splm: Spatial Panel Data Models in R. *Journal of Statistical Software*, 47(1), 1–38.
53. Minor, E. S., & Urban, D. L. (2008). A Graph-Theory Framework for Evaluating Landscape Connectivity and Conservation Planning. *Conservation Biology*, 22(2), 297–307. <https://doi.org/10.1111/j.1523-1739.2007.00871.x>
54. Moilanen, A., & Hanski, I. (1998). Metapopulation dynamics: Effects of habitat quality and landscape structure. *Ecology*, 79(7), 2503–2515. [https://doi.org/10.1890/0012-9658\(1998\)079\[2503:MDEOHQ\]2.0.CO;2](https://doi.org/10.1890/0012-9658(1998)079[2503:MDEOHQ]2.0.CO;2)
55. Moilanen, A., & Nieminen, M. (2002). Simple Connectivity Measures in Spatial Ecology. *Ecology*, 83(4), 1131–1145. [https://doi.org/10.1890/0012-9658\(2002\)083\[1131:SCMISE\]2.0.CO;2](https://doi.org/10.1890/0012-9658(2002)083[1131:SCMISE]2.0.CO;2)
56. Moran, P. A. P. (1950). Notes on Continuous Stochastic Phenomena. *Biometrika*, 37(1/2), 17. <https://doi.org/10.2307/2332142>
57. Neel, M. C. (2008). Patch connectivity and genetic diversity conservation in the federally endangered and narrowly endemic plant species *Astragalus albens* (Fabaceae). *Biological Conservation*, 141(4), 938–955. <https://doi.org/10.1016/j.biocon.2007.12.031>
58. Nobert, B. R., Merrill, E. H., Pybus, M. J., Bollinger, T. K., & Hwang, Y. T. (2016). Landscape connectivity predicts chronic wasting disease risk in Canada. *Journal of Applied Ecology*, 53(5), 1450–1459. <https://doi.org/10.1111/1365-2664.12677>
59. Noss, R. F. (1987). From plant communities to landscapes in conservation inventories: A look at the nature conservancy (USA). *Biological Conservation*, 41(1), 11–37. [https://doi.org/10.1016/0006-3207\(87\)90045-0](https://doi.org/10.1016/0006-3207(87)90045-0)
60. O'Connor, C., Prusinski, M. A., Aldstadt, J., Falco, R. C., Oliver, J., Haight, J., Tober, K., Sporn, L. A., White, J., Brisson, D., & Backenson, P. B. (2024). Assessing the impact of areal unit selection and the modifiable areal unit problem on associative statistics between cases of tick-borne disease and entomological indices. *Journal of Medical Entomology*, 61(2), 331–344. <https://doi.org/10.1093/jme/tjad157>
61. Olson, D. M., Dinerstein, E., Wikramanayake, E. D., Burgess, N. D., Powell, G. V. N., Underwood, E. C., D'amico, J. A., Itoua, I., Strand, H. E., Morrison, J. C., Loucks, C. J., Allnutt, T. F., Ricketts, T. H., Kura, Y., Lamoreux, J. F., Wettengel, W. W., Hedao, P., & Kassem, K. R. (2001). Terrestrial Ecoregions of the World: A New Map of Life on Earth. *BioScience*, 51(11), 933. [https://doi.org/10.1641/0006-3568\(2001\)051\[0933:TEOTWA\]2.0.CO;2](https://doi.org/10.1641/0006-3568(2001)051[0933:TEOTWA]2.0.CO;2)
62. Openshaw, S. (1984). Ecological Fallacies and the Analysis of Areal Census Data. *Environment and Planning A: Economy and Space*, 16(1), 17–31. <https://doi.org/10.1068/a160017>
63. Openshaw, S., & Taylor, P. J. (1979). A million or so correlation coefficients: Three experiments on the modifiable areal unit problem. In *Statistical applications in the spatial sciences* (pp. 127–144). Pion.

64. Pascual-Hortal, L., & Saura, S. (2006). Comparison and development of new graph-based landscape connectivity indices: Towards the prioritization of habitat patches and corridors for conservation. *Landscape Ecology*, 21(7), 959–967. <https://doi.org/10.1007/s10980-006-0013-z>
65. Pebesma, E. (2018). Simple Features for R: Standardized Support for Spatial Vector Data. *The R Journal*, 10(1), 439. <https://doi.org/10.32614/RJ-2018-009>
66. Peterson, M. N., Lopez, R. R., Laurent, E. J., Frank, P. A., Silvy, N. J., & Liu, J. (2005). Wildlife Loss through Domestication: The Case of Endangered Key Deer. *Conservation Biology*, 19(3), 939–944. <https://doi.org/10.1111/j.1523-1739.2005.00069.x>
67. R Core Team. (2022). *R: A language and Environment for Statistical Computing* (4.2.2.) [Computer software]. R Foundation for Statistical Computing. <https://www.R-project.org/>
68. Ricotta, C., Stanisci, A., Avena, G. C., & Blasi, C. (2000). Quantifying the network connectivity of landscape mosaics: A graph-theoretical approach. *Community Ecology*, 1(1), 89–94. <https://doi.org/10.1556/ComEc.1.2000.1.12>
69. Robinson, W. S. (1950). Ecological Correlations and the Behavior of Individuals. *American Sociological Review*, 15(3), 351. <https://doi.org/10.2307/2087176>
70. Rogerson, P. (2015). *Statistical methods for geography: A student's guide* (Fourth Edition). SAGE.
71. Rogerson, P. (2021). *Spatial statistical methods for geography*. SAGE.
72. Rooney, T. P. (2001). Deer impacts on forest ecosystems: A North American perspective. *Forestry*, 74(3), 201–208. <https://doi.org/10.1093/forestry/74.3.201>
73. Saura, S., Bastin, L., Battistella, L., Mandrici, A., & Dubois, G. (2017). Protected areas in the world's ecoregions: How well connected are they? *Ecological Indicators*, 76, 144–158. <https://doi.org/10.1016/j.ecolind.2016.12.047>
74. Saura, S., Bertzky, B., Bastin, L., Battistella, L., Mandrici, A., & Dubois, G. (2018). Protected area connectivity: Shortfalls in global targets and country-level priorities. *Biological Conservation*, 219, 53–67. <https://doi.org/10.1016/j.biocon.2017.12.020>
75. Saura, S., Estreguil, C., Mouton, C., & Rodríguez-Freire, M. (2011). Network analysis to assess landscape connectivity trends: Application to European forests (1990–2000). *Ecological Indicators*, 11(2), 407–416. <https://doi.org/10.1016/j.ecolind.2010.06.011>
76. Saura, S., & Pascual-Hortal, L. (2007). A new habitat availability index to integrate connectivity in landscape conservation planning: Comparison with existing indices and application to a case study. *Landscape and Urban Planning*, 83(2–3), 91–103. <https://doi.org/10.1016/j.landurbplan.2007.03.005>
77. Schmit, J. P., Matthews, E. R., & Brolis, A. (2020). Effects of culling white-tailed deer on tree regeneration and *Microstegium vimineum*, an invasive grass. *Forest Ecology and Management*, 463, 118015. <https://doi.org/10.1016/j.foreco.2020.118015>
78. Tang, W., & Bennett, D. A. (2010). Agent-based Modeling of Animal Movement: A Review: Agent-based modeling of animal movement: a review. *Geography Compass*, 4(7), 682–700. <https://doi.org/10.1111/j.1749-8198.2010.00337.x>

79. Taylor, P. D., Fahrig, L., Henein, K., & Merriam, G. (1993). Connectivity Is a Vital Element of Landscape Structure. *Oikos*, 68(3), 571. <https://doi.org/10.2307/3544927>
80. Tischendorf, L., & Fahrig, L. (2000a). How should we measure landscape connectivity? *Landscape Ecology*, 15(7), 633–641. <https://doi.org/10.1023/A:1008177324187>
81. Tischendorf, L., & Fahrig, L. (2000b). On the usage and measurement of landscape connectivity. *Oikos*, 90(1), 7–19. <https://doi.org/10.1034/j.1600-0706.2000.900102.x>
82. Udvardy, M. (1975). *A classification of the biogeographical provinces of the world. Morges (Switzerland): International Union of Conservation of Nature and Natural Resources. IUCN Occasional Paper no. 18.*
83. Urban, D., & Keitt, T. (2001). LANDSCAPE CONNECTIVITY: A GRAPH-THEORETIC PERSPECTIVE. *Ecology*, 82(5), 1205–1218. [https://doi.org/10.1890/0012-9658\(2001\)082\[1205:LCAGTP\]2.0.CO;2](https://doi.org/10.1890/0012-9658(2001)082[1205:LCAGTP]2.0.CO;2)
84. Urban, D. L., Minor, E. S., Treml, E. A., & Schick, R. S. (2009). Graph models of habitat mosaics. *Ecology Letters*, 12(3), 260–273. <https://doi.org/10.1111/j.1461-0248.2008.01271.x>
85. Urban, D. L., O'Neill, R. V., & Shugart, H. H. (1987). Landscape Ecology. *BioScience*, 37(2), 119–127. <https://doi.org/10.2307/1310366>
86. VanAcker, M. C., DeNicola, V. L., DeNicola, A. J., Aucoin, S. G., Simon, R., Toal, K. L., Diuk-Wasser, M. A., & Cagnacci, F. (2023). Resource selection by New York City deer reveals the effective interface between wildlife, zoonotic hazards and humans. *Ecology Letters*, ele.14326. <https://doi.org/10.1111/ele.14326>
87. VanAcker, M. C., Little, E. A. H., Molaei, G., Bajwa, W. I., & Diuk-Wasser, M. A. (2019). Enhancement of Risk for Lyme Disease by Landscape Connectivity, New York, New York, USA. *Emerging Infectious Diseases*, 25(6), 1136–1143. <https://doi.org/10.3201/eid2506.181741>
88. Vos, C. C., Antonisse-De Jong, A. G., Goedhart, P. W., & Smulders, M. J. M. (2001). Genetic similarity as a measure for connectivity between fragmented populations of the moor frog (*Rana arvalis*). *Heredity*, 86(5), 598–608. <https://doi.org/10.1046/j.1365-2540.2001.00865.x>
89. Waser, P. M., & Strobeck, C. (1998). Genetic signatures of interpopulation dispersal. *Trends in Ecology & Evolution*, 13(2), 43–44. [https://doi.org/10.1016/S0169-5347\(97\)01255-X](https://doi.org/10.1016/S0169-5347(97)01255-X)
90. Whitlock, M. C., & McCauley, D. E. (1999). Indirect measures of gene flow and migration: $F_{ST} \neq 1/(4Nm+1)$. *Heredity*, 82(2), 117–125. <https://doi.org/10.1038/sj.hdy.6884960>
91. Wickham, H. (2016). *ggplot2: Elegant Graphics for Data Analysis* (2nd ed. 2016). Springer International Publishing: Imprint: Springer. <https://doi.org/10.1007/978-3-319-24277-4>
92. Wiens, J. A. (1989). Spatial Scaling in Ecology. *Functional Ecology*, 3(4), 385. <https://doi.org/10.2307/2389612>
93. Wiens, J. A., & Milne, B. T. (1989). Scaling of “landscapes” in landscape ecology, or, landscape ecology from a beetle’s perspective. *Landscape Ecology*, 3(2), 87–96. <https://doi.org/10.1007/BF00131172>

94. Williams, D. M., Dechen Quinn, A. C., & Porter, W. F. (2012). Landscape effects on scales of movement by white-tailed deer in an agricultural–forest matrix. *Landscape Ecology*, 27(1), 45–57. <https://doi.org/10.1007/s10980-011-9664-5>

95. Wood, S. N. (2011). Fast Stable Restricted Maximum Likelihood and Marginal Likelihood Estimation of Semiparametric Generalized Linear Models. *Journal of the Royal Statistical Society Series B: Statistical Methodology*, 73(1), 3–36. <https://doi.org/10.1111/j.1467-9868.2010.00749.x>

Table

Table 5 is available in the Supplementary Files section.

Figures

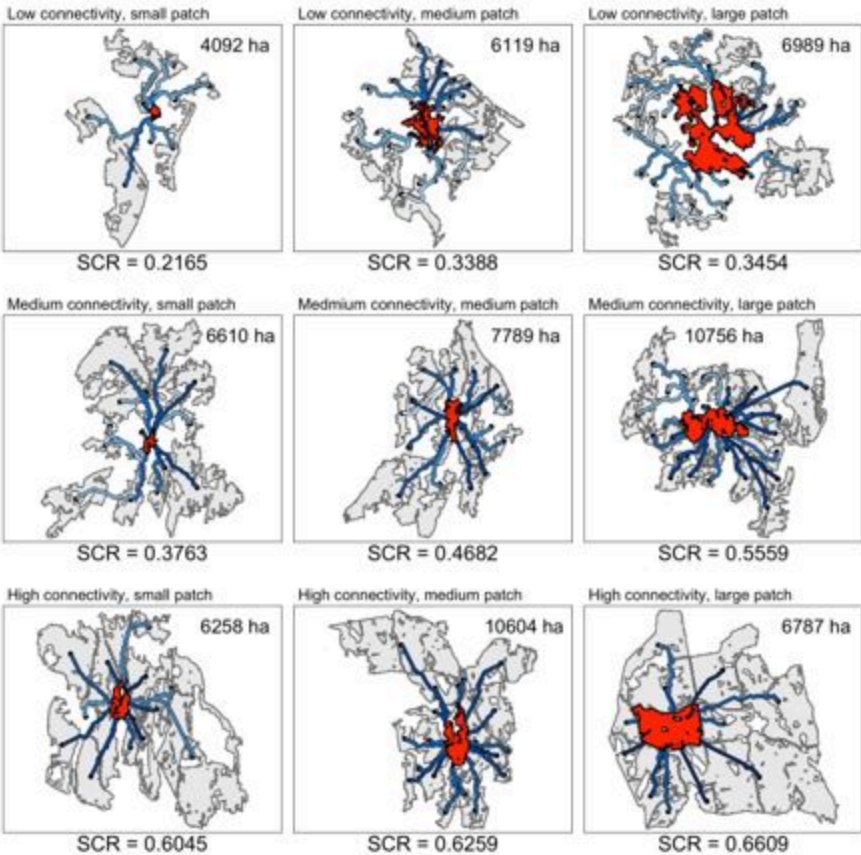


Figure 1: Nine examples of the Sinuous Connection Reduction index (SCR) taken from a NYS County. Focal patches are shown in red. Total area of each map shown in hectares within insets. Focal patch sizes (a_i) increase as columns go left to right, and inverse sinuosity-weighted adjacent patch sizes ($\sum_{j=1}^n s_{ij}^* a_j$) increase as rows go top to bottom. Least-cost paths are shown, where darker blues indicate a more direct path (s_{ij}^*).

Figure 1

See image above for figure legend

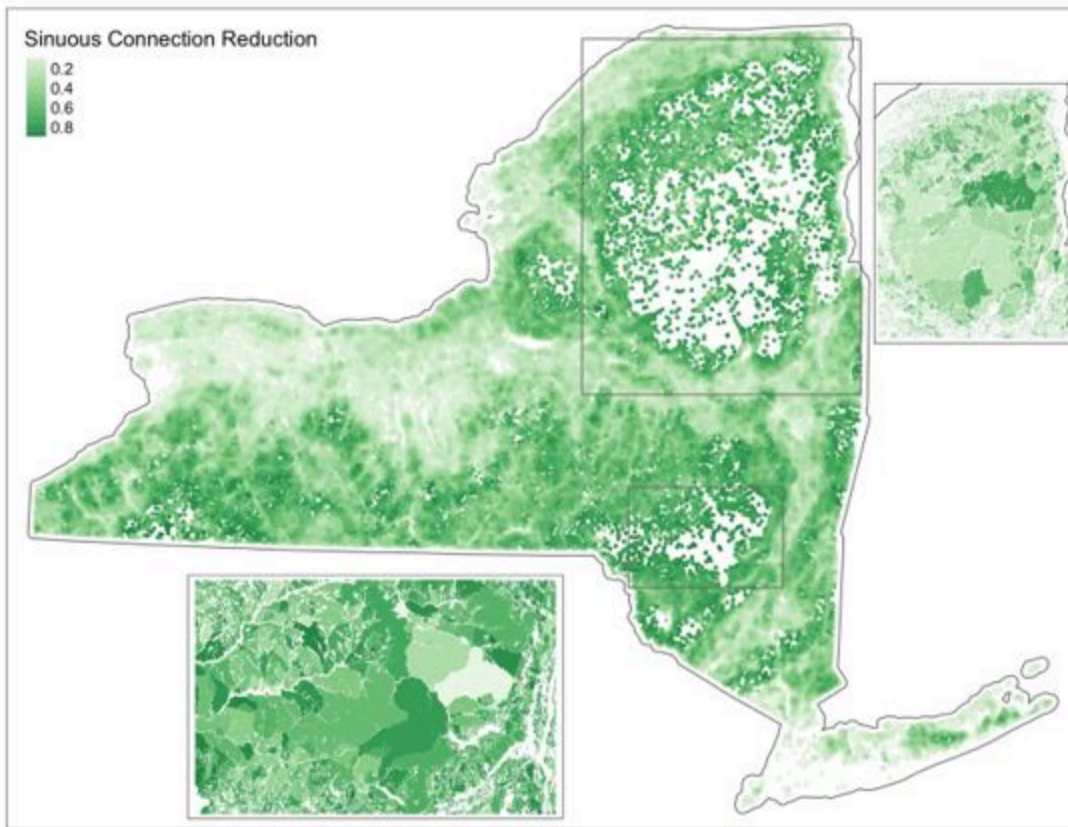


Figure 2

Maps displaying calculated values for the Sinuous Connection Reduction index (SCR) for 66,295 forest patches in NYS. Centroids of forest patches are shown in main map. Forest patch polygons of the Adirondack and Catskill parks are shown in map insets.

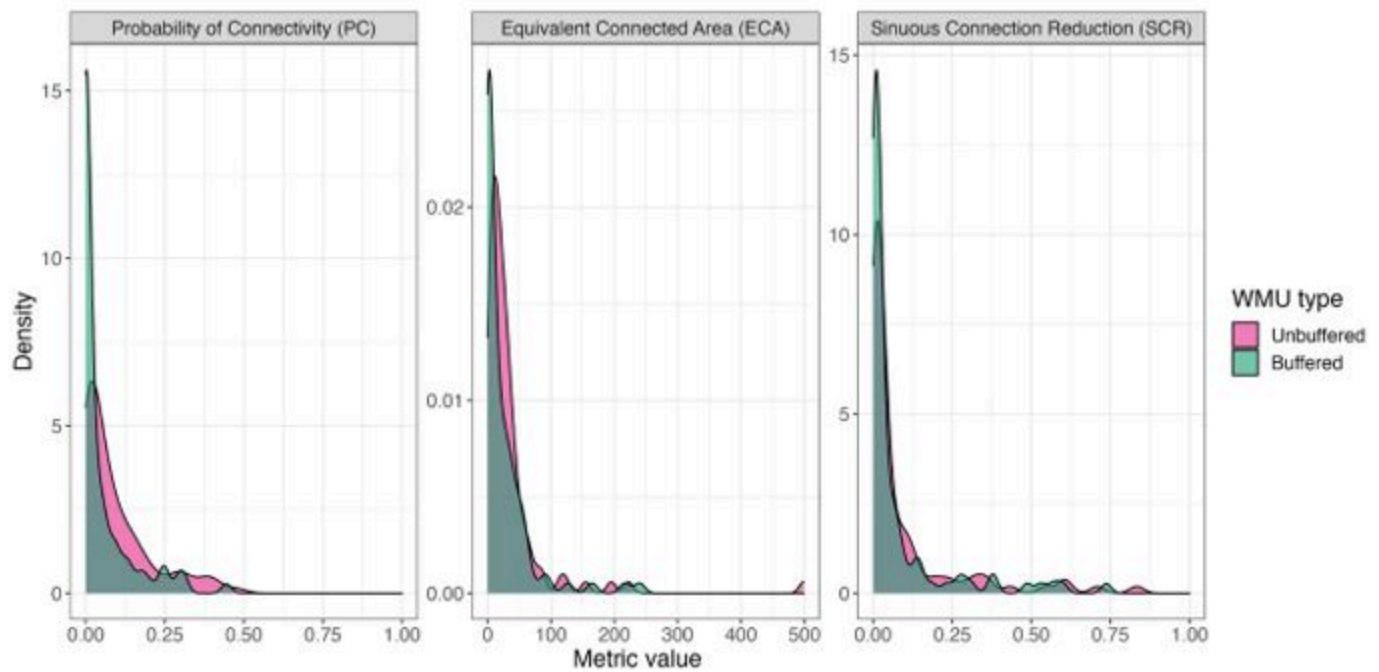


Figure 3

Frequency distributions of the Probability of Connectivity index, Equivalent Connected Area (ECA), and Sinuous Connection Reduction index for white-tailed deer connectivity in 92 Wildlife Management Units in NYS. Values for ECA are divided by 1,000 to fit labels in figure.

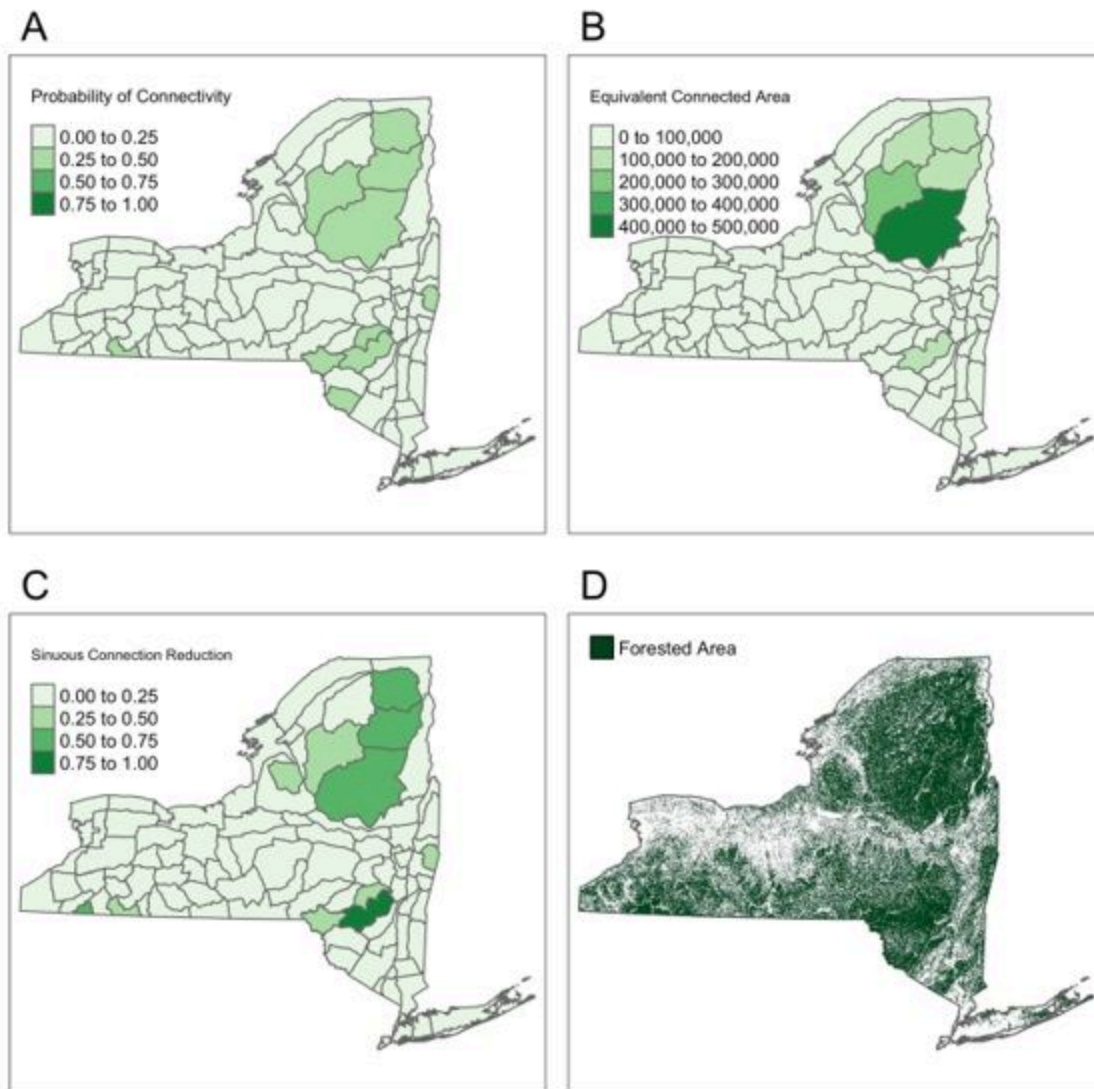


Figure 4

Choropleth maps of A) Probability of Connectivity index, B) Equivalent Connected Area, and C) Sinuous Connection Reduction (SCR) index for white-tailed deer connectivity in 92 wildlife management units in NYS. D) Coniferous, deciduous and mixed forest classes gathered from the National Land Cover Database (NLCD) 2019 Land Cover Dataset at 30-meter resolution.

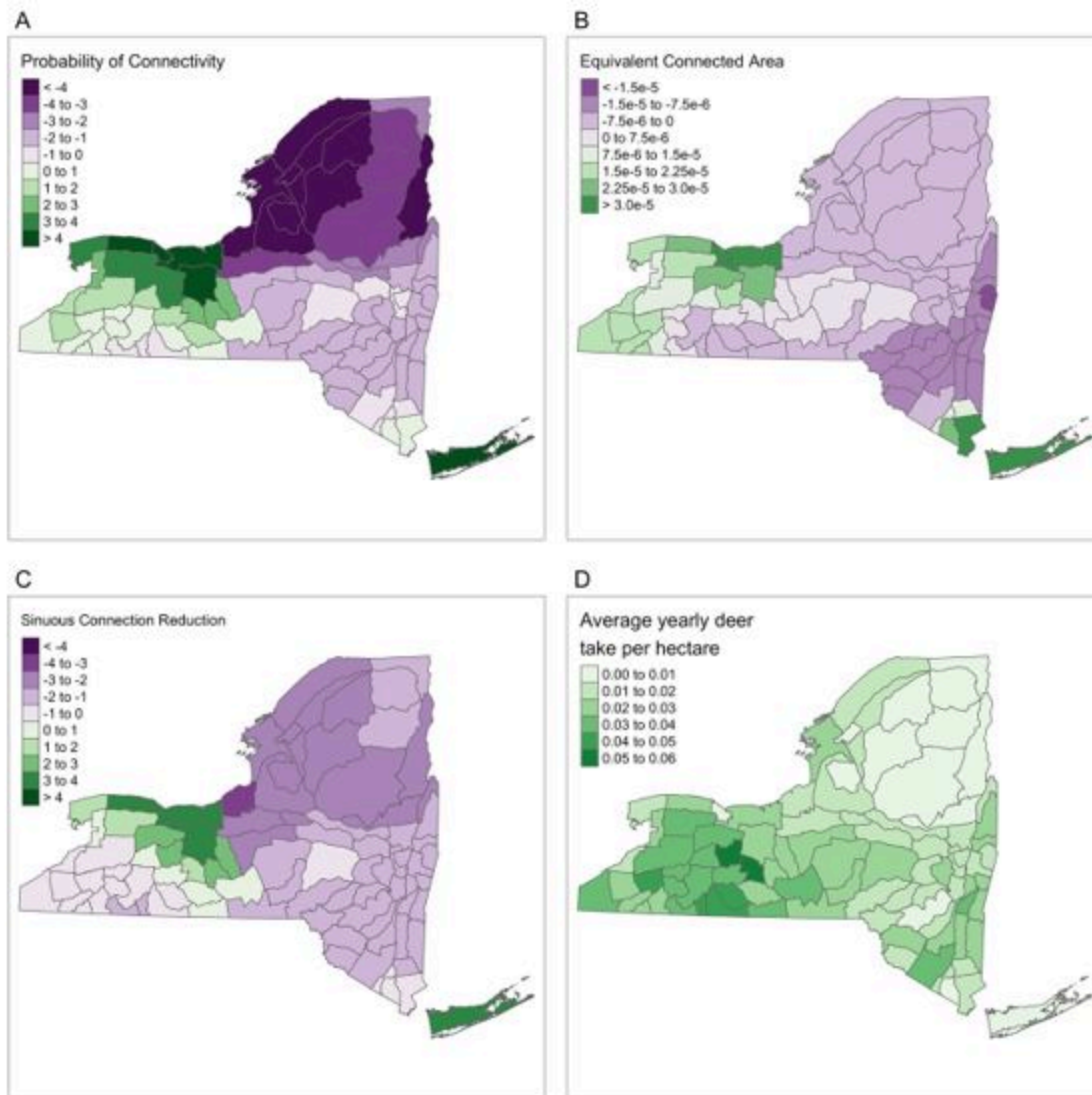


Figure 5

Average β coefficients for wildlife management units (1988 – 2021) from geographically weighted regression models estimating the relationship between estimates of white-tailed deer connectivity A) Probability of Connectivity index, B) Equivalent Connected Area metrics, and C) Sinuous Connection Reduction index and D) Deer take per hectare.

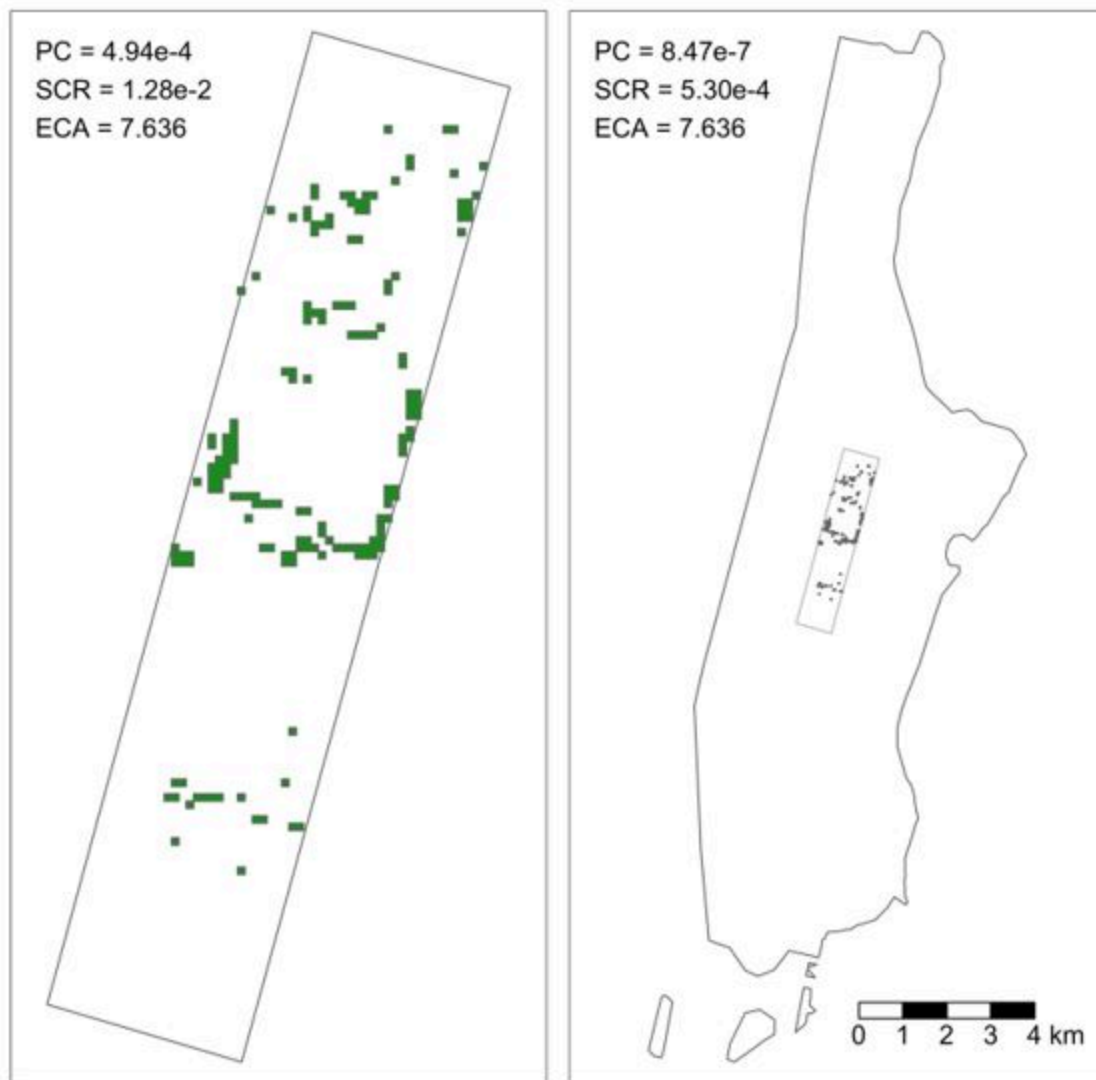


Figure 6

Forest patches within Central Park boundaries (left) in Manhattan, New York City (right). Probability of Connectivity (PC) and Sinuous Connection Reduction (SCR) indices and Equivalent Connected Area (ECA) metrics are shown in the top left of both maps. When widening the study area in the calculation from only Central Park to all of Manhattan, the PC and SCR indices decrease while the ECA remains the same. Only forest patches in Central Park are included in both calculations.

Supplementary Files

This is a list of supplementary files associated with this preprint. Click to download.

- [Table5.xlsx](#)
- [FigureS1.tiff](#)
- [FigureS2.tiff](#)